Chapter 8
Types of Confocal Instruments: Basic Principles and Advantages and Disadvantages

John Fuseler, W. Gray (Jay) Jerome, and Robert L. Price

8.1 Introduction

As noted in the Historical Perspectives section of Chap. 1, several types of confocal laser scanning microscopes (CLSM) have been introduced over the years. At this point, these can be broken down into four basic categories: single-photon point-scanning confocal systems, multiphoton (nonlinear) point-scanning confocal systems, spinning disk confocal microscopes, and super-resolution systems. New developments are continually being added to the hardware and software of these microscopes to improve their performance, but the majority of confocal systems will fall into one of these groups. Table 8.1 compares many of the features of single-photon, multiphoton, and spinning disk systems.

J. Fuseler
Department of Pathology, Microbiology and Immunology, University of South Carolina School of Medicine, Columbia, SC, USA

W. G. Jerome (✉)
Department of Pathology, Microbiology and Immunology, Vanderbilt University School of Medicine, Nashville, TN, USA
e-mail: Jay.Jerome@Vanderbilt.edu

R. L. Price
Department of Cell Biology and Anatomy, University of South Carolina School of Medicine, Columbia, SC, USA
e-mail: Bob.Price@uscmed.sc.edu

W. G. Jerome, R. L. Price (eds.), *Basic Confocal Microscopy*,
https://doi.org/10.1007/978-3-319-97454-5_8

Table 8.1 Comparison of several characteristics of single-photon CSLM, multiphoton CSLM, and spinning disk confocal systems

Characteristic	Single-photon CSLM	Multiphoton CSLM	Spinning disk
Photon source	High-intensity short-wavelength lasers	Adjustable lasers capable of long wavelengths (IR)	Lasers, mercury, xenon, or metal-halide lamps
Acquisition speed	At full-resolution and frame size scan speeds can be several seconds per frame. Fast scans of regions of interest at reduced resolution available on some systems	Similar limitations as single photon	Rapid, high frame rates of 20^{+} frames per second
X-Y resolution	Up to 4096 × 4096 on some systems	Up to 4096 × 4096 on some systems	Depends on CCD elements and binning
Z- resolution	~0.6 μm optimum based on 63× NA1.4 oil objective with pinhole at 1 airy unit		Typically fixed (micro-lenses)
Detectors	Photomultiplier tubes (PMTs) or related systems (see Chap. 7)	Photomultiplier tubes (PMT) or related systems (see Chap. 7)	Charge-coupled device (CCD) or complementary metal-oxide semiconductors (CMOS)
Multi-channel imaging	Simultaneous or sequential	Simultaneous or sequential	Sequential
Photobleaching and phototoxicity	May be problematic	Typically not a problem	Reduced based on fast imaging parameters
Region-specific bleaching	Possible on instruments that allow region of interest control of excitation areas	Possible on instruments that allow region of interest control of excitation areas	Requires additional hardware available for some systems
Depth of imaging	Limited based on optics and wavelength of laser	Greatly improved over single photon based on long-wavelength excitation	Limited

8.2 Single-Photon Point-Scanning Confocal Microscopes

These instruments, by far, represent the majority of confocal microscopes in today's laboratories and include basic instruments with two or three lasers all the way up to very advanced spectral imaging microscopes such as the Zeiss LSM 880, Leica SP8, Nikon A1^{+}, and Olympus Fluoview FV3000 instruments. Resonant scanning systems, designed to increase the rate of scanning for live cell imaging, also fall within this group of instruments.

Figure 8.1 illustrates a simplified diagram of the path that photons take prior to and after interaction with the specimen in a single-photon point-scanning confocal

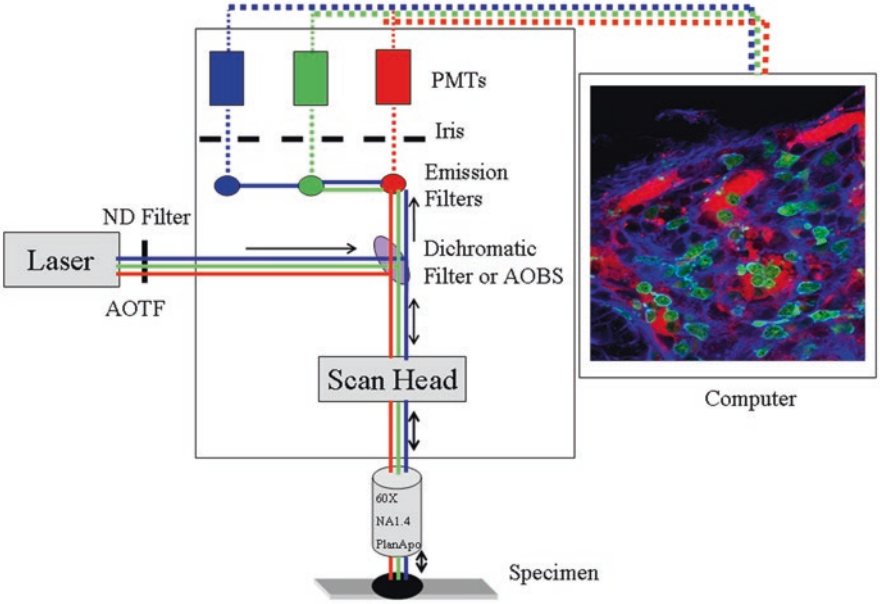

Fig. 8.1 Generalized diagram of the mechanism for sequentially exciting and collecting signal from a sample labeled with three fluorochromes

system. After exiting the laser, photons pass through a neutral density filter or an acousto-optical tunable filter (AOTF) that allows control of the laser intensity that contacts the specimen. The laser beam then passes through a dichroic filter present in most confocal systems or an acousto-optical beam splitter (AOBS) in Leica microscopes. This filtering mechanism separates the higher-energy short-wavelength excitation photons from the lower-energy long-wavelength photons emitted from the specimen. The laser beam then passes through the scan head and objective lens before interacting with the specimen. As the laser is scanned across the specimen, fluorophores are excited resulting in emission of photons from the specimen.

Photons emitted from the specimen take the reverse path (epifluorescence microscopes) of the excitation photons and first pass through the objective and then through the dichroic filter or AOBS. In the example shown in Fig. 8.1 blue, green and red laser lines are used to excite the specimen. Emitted photons are then sorted by placing a dichroic mirror and long pass filter in front of the first detector, so only red light passes through to the detector. Shorter wavelengths are redirected. In most laser scanning confocal systems, the detector is usually a photomultiplier tube (PMT), although many systems are now incorporating higher sensitivity GaAsP detectors (Sect. 7.3.1). Many laser scanning systems, such as the one depicted in Fig. 8.1, have multiple detectors, and in newer systems, combinations of PMTs and GaAsP detectors are becoming common. Confocal detectors do not recognize color; they collect and record photons of all wavelengths. It is the combination of filters between the specimen and detector that allow us to assign specific colors

(wavelengths) to the detected photons. In the case of a three-PMT detector system, when the long (red) wavelengths are passed on to a PMT, the remaining shorter wavelengths (green and blue) are redirected by the dichroic or AOBS to other detectors. A second dichroic directs the green wavelengths through a band-pass filter to a second detector, while shorter (blue) wavelengths are redirected to a third detector, and long (any remaining red) wavelengths are blocked and do not progress further. The third PMT receives only the short wavelength (blue) light left in the emitted light. Combinations of filters and detectors can be used in this manner to sort multiple wavelengths of light.

When the first edition of this book was published, spectral detectors were a relatively new development in laser scanning confocal microscopy. Today spectral detectors are much more common and can be found on many confocal systems. Spectral detectors separate the light into its component wavelengths and have the ability to detect very narrow ranges (10 nm or less) of light, allowing the microscopist to more precisely analyze the spectrum of wavelengths emitted from a specimen. However, in practice, selection of too narrow a band of light results in a poor signal-to-noise ratio (SNR), so often bands of 20 nm or more are used for imaging.

When planning an experiment, it is very important to know the filters available on the instrument before selecting a combination of fluorochromes to use for multiple labeling experiments. Improper selection of fluorochromes and filters may result in problems such as bleed through and poor signal levels as discussed in Chap. 3.

Prior to reaching the detector, a pinhole (aperture, iris) is placed in the light path at the light beam's focal point. This is a very critical component of a confocal microscope because this is the point where out-of-focus light is separated from light coming from the focal plane. In some systems, a pinhole is placed in front of each detector, while in others, a single pinhole is used to remove out-of-focus light prior to the photons being sorted and sent to the various detectors. Proper use of the pinhole is important in achieving the essential feature of confocal microscopy so that only light from the focal point of the objective is used in image formation. Thus, *the focused point of the specimen and detection of the signal is in conjugate focus (confocal)* resulting in the improved resolution, contrast, and SNR characteristic of confocal images. Once the emission photons are sorted, the information is converted to a digital image as discussed in Chaps. 6 and 7.

The ability to remove out-of-focus light from the image and the use of high-resolution and very sensitive detection devices, along with microscope stages that can be tightly controlled in movement in the Z direction, provide the capability to collect a series (Z-series) of in-focus images throughout the depth of a specimen. This feature allows high-resolution scanning in the X, Y, and Z axes for the collection and reconstruction of true three-dimensional data sets, which is a major advantage of CSLM systems when compared to widefield fluorescence systems (Fig. 1.4).

Choices made by the operator at each point along the optical path affect both the amount of specimen damage that may occur and image quality. Factors that increase the intensity of the laser contacting the specimen or the length of time the laser remains in contact with a point in the specimen will increase the number of photons (signal) available for formation of the image but will result in increased specimen

damage in the form of quenching of fluorescent reagents and/or cell death if imaging live cells. Other factors, such as increasing the diameter of the pinhole, will alter image parameters such as SNR and resolution but will not directly affect specimen damage since interaction of the laser with the specimen has been completed. Understanding the multiple compromises made in collection of an image is essential since nearly every change made in operating parameters will affect specimen damage, image quality, or both. Chapter 9 provides details on how the microscope should be set up to maximize specimen preservation and image quality and discusses many of the compromises in imaging that must be made.

8.2.1 Limitations of Single-Photon Confocal Systems: Cost

An obvious limitation in the use of confocal microscopes is the cost of acquisition and maintenance. Depending on configuration, commercially available basic instruments often approach $300–400 K, and advanced systems very often exceed $1 M in cost. Instruments of this magnitude typically require service contracts that are in the neighborhood of $20–25 K per year for basic instruments and often more than $50 K per year for high-end instrumentation. For this reason most systems are placed in core facilities or within groups of well-funded investigators.

8.2.2 Limitations of Single-Photon Confocal Systems: Difficult to Operate

Confocal microscopes are also relatively difficult to operate requiring, at a minimum, a part-time operator for routine maintenance and training of new users. The importance of a skilled operator for training cannot be underestimated as the operating parameters of a confocal system can easily be set up incorrectly resulting in the collection of data that does not accurately represent the sample. This can lead to artifacts with regard to the size of structures, three-dimensional reconstructions, and interpretation of fluorochrome co-localization as discussed in Chaps. 10 and 11. Helping the microscopists identify these critical parameters and understanding how to properly set them are key goals of this book.

8.2.3 Limitations of Single-Photon Confocal Systems: Speed of Acquisition

Another distinct disadvantage of the point-scanning systems is that image acquisition is a relatively slow process. In these systems the lasers are scanned across the specimen in an X-Y direction by galvanometer mirrors in the scan head. The speed of the mirrors is limited which in turn limits the rate the laser can be rastered across

the surface of the sample. As a result, it often takes 2–3 s to collect a single frame. If the goal of the experiment is to image rapidly occurring events such as a calcium flux, imaging must be completed in milliseconds rather than seconds.

Spinning disk (discussed in detail in Sect. 8.4), slit scanning, and resonant scanning systems are modifications of confocal technology that have been developed to address the problem of slow image acquisition. Slit scanning systems use a wedge of excitation light rather than a point of light and slit apertures rather than pinhole apertures to decrease the time required to scan a sample. Nikon has also produced a Swept Field System that is a combination of point and slit scanning technology so that the option of high-resolution or high-speed imaging can be selected based on the goal of the experiment.

In high-speed resonant scanning systems, rather than rastering the beam, the galvanometer mirrors vibrate at a fixed frequency to rapidly move the beam across the specimen. This significantly increases the speed of scanning and results in scans that take approximately 125 μs. At this speed resonant scanners are capable of collecting 30 frames or more per second which is fast enough to record most events in live cell imaging. The speed of acquisition also reduces many of the phototoxicity problems associated with using high-intensity lasers since exposure is for a very short period of time.

8.2.4 Limitations of Single-Photon Confocal Systems: Photobleaching and Phototoxicity

Associated with the problem of slow speed of image acquisition are the problems of photobleaching of fixed samples and phototoxicity if imaging live cells. As noted above, the high-intensity lasers of single-photon systems may result in considerable photodamage resulting in photobleaching of fluorescent dyes and the death of cells if imaging living samples. Both multiphoton and spinning disk systems discussed below minimize these types of damage.

Much of the photobleaching problem with single-photon CSLM systems is that, as is the case with epifluorescence microscopes, the entire volume of the specimen is exposed to the high-intensity laser. This means that as the focal plane of the specimen is being scanned, the optical planes above and below the focal plane are also exposed to the high-intensity photons of the laser (Fig. 8.2). This may result in specimen damage throughout the specimen. In addition, emitted photons from the out-of-focus planes can potentially contribute to the final image resulting in decreased resolution and image quality. As described in Sect. 8.3, multiphoton excitation can help minimize the beam interaction with fluorophores in the out-of-focus planes.

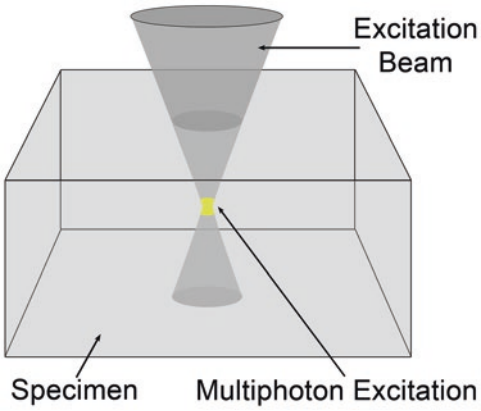

Fig. 8.2 The photon density is only high enough at the focal point of the excitation beam for two-photon absorption to occur. Fluorophores above and below the plane of focus remain unexcited

8.2.5 Limitations of Single-Photon Confocal Systems: Resolution

Resolution was discussed extensively in Sect. 7.2 and the equation for calculation of resolution given in Eq. 7.1. Traditionally the resolution obtained with a confocal microscope is typically compared to that of a widefield epifluorescence system and is therefore considered to be excellent. However, even with confocal systems, the imaging source is comprised of light which has a long wavelength (λ) compared to electrons, and with the introduction of several super-resolution instruments, realization of resolution limitations in traditional confocal microscopy has become more evident.

The diffraction limitations on resolution when using photons as the imaging source were important factors in development of several super-resolution light microscopy techniques that received the 2014 Nobel Prize in Chemistry for Drs. Betzig, Hell, and Moerner (https://www.nobelprize.org/nobel_prizes/chemistry/laureates/2014/press.html). A full discussion of super-resolution techniques goes beyond the topic of basic confocal microscopy addressed here, but a brief introduction to the technique and reference to several reviews (Leung and Chou 2011; Yamanaka et al. 2014; Sydor et al. 2015; Laine et al. 2016) that discuss the topic are warranted. The importance of super-resolution techniques is easily recognized by examining the number of recent publications using the technology. A March 2018 search of NIH PubMed using "super-resolution microscopy" as the keyword search term showed a rapid growth in use of the technology as reported in publications (Fig. 8.3).

Most super-resolution techniques reduce the point spread function (PSF) generated from a fluorochrome and deconvolution to supersede diffraction-limited resolution. Reduction of the PSF may be by use of lasers to deactivate part of the PSF as in STED (stimulated emission depletion microscopy) and ground-state depletion (GSD) microscopy, through the use of sparsely labeled photoactivatable fluorochromes such as photoactivated localization (PALM) and stochastic optical recon-

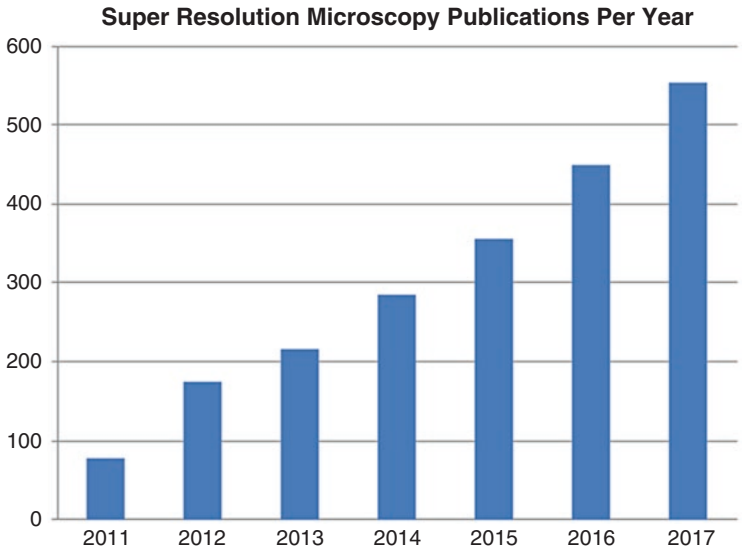

Fig. 8.3 Chart showing the rapid increase in super-resolution papers published since 2011

struction (STORM) microscopy, or through computational reconstruction of several images as in structured illumination microscopy (SIM). There are also many variations of these and other techniques that are being developed to circumvent the PSF. These include combinations of techniques such as saturated SIM (SSIM) that uses a combination of computation reconstruction in conjunction with the principle of STED. All of these techniques are reviewed in detail in the reviews cited above.

The above techniques all achieve resolution in the range of tens of nanometers and have various limitations such as the use of specific lasers and or fluorochromes. Several manufacturers have developed systems that improve on the practical resolution limits (200 nm or more) of confocal microscopy and achieve resolution in the range of 140 nm. A major advantage of these systems, such as the Zeiss Airyscan, the Leica HyVolution, and the Olympus Fluoview 3000-OSR is that they can often be used with specimens prepared with standard specimen preparation fluorochromes and protocols previously discussed. The primary advances in technology used in these enhanced resolution systems are high sensitivity GaAsP and Leica HyD detectors that require very little signal to saturate. The high sensitivity allows the pinhole to be decreased to approximately 0.7 Airy units (AU) improving resolution from the standard optimum setting of 1 AU. In combination with deconvolution, the reduced pinhole size attains the improved resolution.

The significance of super-resolution techniques, whether it is true super resolution in the range of 50 nanometers or less or in the range of 140 nanometers, is our understanding of biomolecular mechanisms. Many co-localization studies that were previously performed with standard confocal imaging systems that experienced diffraction-limited resolution in the range of 200 nm or more must now be questioned. Figure 1.4 showed a comparison of traditional confocal and Airyscan images

from the brain hippocampus. Figures 8.4 and 8.5 show super-resolution images that further illustrate the improved resolution associated with PALM and STORM instruments. Structures that previously could not be resolved due to the PSF are now seen as distinct structures.

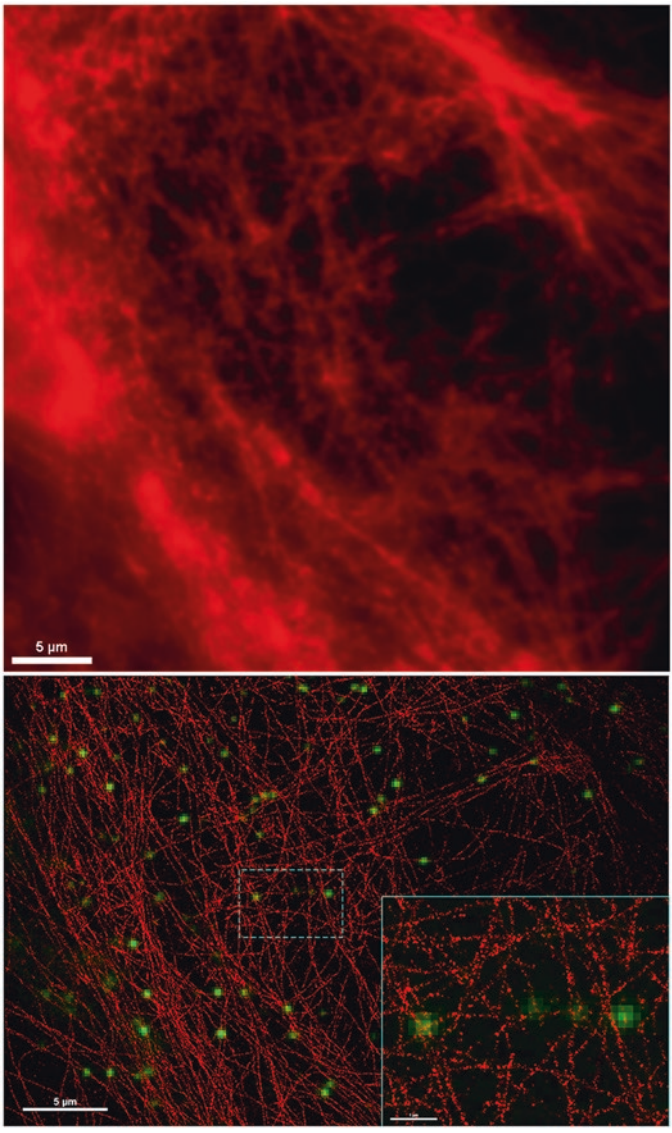

Fig. 8.4 Comparison of widefield (top) and direct stochastic optical reconstruction microscopy (dSTORM) images showing increased resolution of alpha-tubulin labeling in CO-1 cells. Images provided courtesy of John Allen from Nikon and Bryan Mills and Meagan Postema from Vanderbilt University

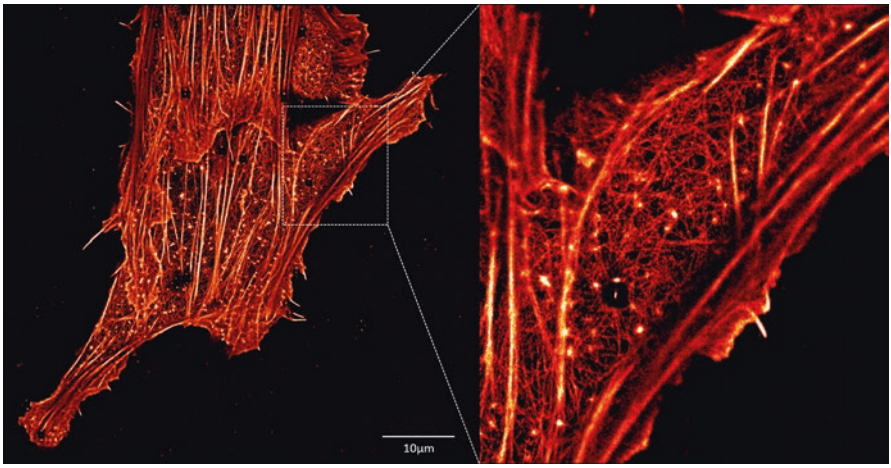

Fig. 8.5 Super-resolution interferometric Photoactivation and Localization Microscopy (iPALM) image of actin in NIH-3 T3 cells. Images provided courtesy of Teng-Leong Chew: https://www.aicjanelia.org/ipalm-techspecs

Table 8.2 Comparison of the wavelengths of visible light available for confocal imaging and electrons when an electron microscope is operated at 60 kV

Color/source	Wavelength in nm
Electrons	0.005
Violet	380–450
Blue	450–490
Green	490–560
Yellow	560–590
Orange	590–630
Red	630–760

Even with the development of super-resolution imaging techniques, the use of photons continues to limit the ultimate resolution that can be obtained with light microscopy based on the physics of photon wavelengths. In comparison, the resolution available with an electron microscope is orders of magnitude higher. As shown in Table 8.2, the wavelengths of visible light are significantly longer than those of electrons with the shortest wavelength of light typically used in confocal microscopy being ~ 400 nm. When operated at an accelerating voltage of 60 kV, which is relatively low for transmission electron microscopy (TEM), the wavelength of electrons is 0.005 nm. When these wavelength values are inserted into Eq. 7.1 for resolution, the theoretical resolution of a TEM operated at 60 kV is 0.005 nm, although in practice due to astigmatism and spherical and chromatic aberrations the actual resolution is closer to 0.1 nm. This is still an order of magnitude better than the reported 10 nm resolution obtainable with some super-resolution microscopes. Figure 8.6 illustrates the difference in available resolution when imaging cardiac myocytes labeled with fluorochromes by CSLM and with colloidal gold particle

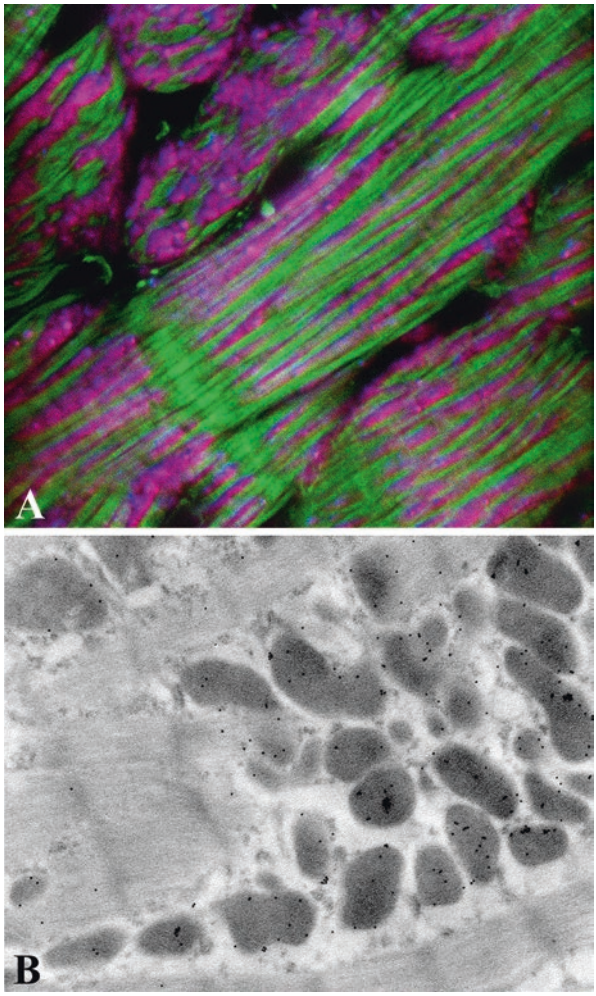

Fig. 8.6 Comparison of resolution levels with confocal microscopy (**a**) and transmission electron microscopy (**b**). In (**a**), cardiac myocytes are labeled with phalloidin for f-actin (green), MitoTracker (red), and cytochrome C (blue). Cytochrome C is primarily localized to the mitochondria creating the purple color. In (**b**), even with minimal fixation for subsequent immunocytochemistry, actin fibers can be seen in the cardiac myocytes cytochrome C labeled with 10 nm colloidal gold particles show clear localization in the mitochondria

labeling for imaging by TEM. While specimen preparation for immunocytochemistry at the TEM level of resolution is much more difficult than for confocal microscopy, TEM does provide an essential correlative technology to confocal and super-resolution imaging for high-resolution labeling. Additional details and examples of probes that can be used for both CSLM and electron microscopy for correlative studies were presented in Chap. 5.

8.3 Multiphoton Point-Scanning Confocal Systems

As described in Chap. 2, in addition to excitation by a single photon, fluorochromes can be excited if more than one photon is absorbed simultaneously. Although the potential for multiple absorptions of photons with different energies exists, in

practice, it is usually absorption of two photons of similar energies that is most often exploited. Thus, for the remainder of this section, we will focus on two-photon excitation microscopy. The quantum possibility of two-photon absorption was first proposed by Maria Göppert-Mayer in 1931. However, technical limitations delayed a practical test of the theory. As will become clear later in this section, the invention of appropriate lasers provided the needed excitation source for two-photon excitation. With the development of these laser microcopy systems has come the development of two-photon microscopy based on the pioneering work of Winfried Denk and others in Watt Webb's laboratory at Cornell University (Denk et al. 1990).

The general theory of two-photon excitation is relatively simple. The excitation of a fluorochrome requires the absorption of energy from an impinging photon. Once energy is absorbed, the fluorochrome is refractory to additional energy absorption for a finite amount of time. However, if two photons arrive within the absorption cross section of the fluorochrome simultaneously, the energies of both can be absorbed as long as their combined energies match the energy needed to excite the fluorochrome. In this respect, simultaneously means within about 10^{-18} s. Thus, the absorption of two photons of lower energy is roughly equivalent to the absorption of a single photon of higher energy. Since the energy of a photon is inversely proportional to its wavelength, the two lower-energy photons should be about twice the wavelength of the corresponding single higher-energy photon. For example, a fluorophore that normally absorbs at 400 nm can also be excited by two photons of wavelength about 800 nm. Of course, neither of the 800 nm photons alone will have sufficient energy to excite the fluorochrome, so unless both photons arrive essentially simultaneously, the fluorochrome will not be excited.

Because the two-photon excitation requires simultaneous absorption, the generation of fluorescence emission depends on the square of the excitation intensity. In practice, the probability of two photons falling within the excitation cross section of a fluorophore is very small except at the focal point of the excitation beam. At this point, the photons are sufficiently crowded together so that a significant number of two-photon excitations occur. This results in localized excitation within a narrow region around the focal point of the excitation beam as depicted in Fig. 2.4. The fact that a highly focused beam of light greatly increases the probability of two-photon excitation means that the scanning confocal microscope would be an ideal tool for two-photon imaging.

The probability that two photons will hit a fluorochrome simultaneously and be absorbed is dependent upon the localized photon density. The density required for two-photon absorption is estimated to be about a million times greater than the density required for single-photon absorption. Thus, two-photon excitation requires very high photon densities. Unlike arc lamps, high-power lasers can provide sufficient photons for two-photon excitation. However, as discussed throughout this book, overly high excitation fluxes can damage both specimen and fluorophore. To get around this, the laser excitation for two-photon excitation is pulsed. In this way, very high photon densities are delivered during the pulse, but the average laser energy over time is low (Denk et al. 1995). Pulse durations are ultrashort ranging from around 100 femtoseconds to 1 picosecond with duty cycles (pulse duration

divided by time between pulses) of about 10^{-5}. This is accomplished using mode-locked lasers. Although short, the pulses are still longer than the time scale of absorption events (~10^{-18} s), and so two-photon excitation is facilitated.

Several distinct advantages accrue from two-photon excitation. Since a signal is only generated at the focal point, there is no fluorescence from the out-of-focus planes. This means that the pinhole can be dispensed with in cases where you need to maximize signal. However, better resolution is still obtained by using a confocal pinhole (Gauderon et al. 1999), and so, in practice, it is useful to use an optimized pinhole unless emission intensity is limiting.

An additional advantage of two-photon excitation related to the localized excitation is that by limiting excitation to the focal plane, two-photon excitation can decrease excitation-induced specimen damage. With single-photon excitation, the entire beam path (Fig. 8.2) within the specimen is subject to potential specimen damage and photobleaching (discussed in detail in Chap. 9). In contrast, with two-photon excitation, only the small focal volume is excited. Damage and photobleaching are limited to this small excitation region. This is of limited utility if you are only imaging a single plane, but it is a tremendous advantage when collecting a stack of focal planes for 3-D reconstructions. With single-photon excitation, fluorochromes above and below the focal plane are also excited. Thus, with multiple passes, each fluorochrome is excited multiple times, and the probability of specimen damage or photobleaching is increased. However, with multiphoton excitation, each fluorochrome is excited only once. Moreover, since there is no out-of-focus absorption, more of the excitation beam reaches the plane of focus and is available to excite fluorophores. This can lead to a 2–three-fold increase in the depth of tissue that can be successfully imaged (Centonze and White 1998). Finally, the two-photon excitation wavelengths used are, by necessity, longer wavelengths, usually in the red to far-red range. These wavelengths of light have the ability to penetrate deeper into wet tissue and produce less tissue damage than shorter wavelengths. Added together, these benefits mean that two-photon excitation provides a very distinct advantage for imaging thick living tissue (Piston 1999).

Of course, all of the advantages of multiphoton excitation are negated if the specimen is prepared incorrectly or the microscope is not set up to maximally exploit the multiphoton capabilities. Chapters 4, 5 and 9 discuss proper specimen preparation and optimization of microscope parameters. Here we will only point out two important considerations which are sometimes overlooked when doing two-photon imaging of live material. The first is matching refractive indices. Using the PSF of a fluorescent bead to measure effective beam penetration, Gerritsen and deGrauw (1999) showed that two-photon excitation allowed imaging at much greater depths compared to single-photon laser scanning confocal, but this advantage was greatly reduced if oil immersion optics were employed. The degradation of the image was due to chromatic aberration introduced because of refractive index mismatches between oil and the essentially water environment of the specimen. In contrast, the advantages of two-photon excitation were maximally exploited when water-immersion optics were used.

The second mistake that one should be diligent to avoid is using the wrong optics. Since two-photon excitation involves long wavelength photons, the objective lens (when using an epifluorescence setup) must be suited to using far-red and infrared light. Ideally, the lens should have high transmittance in these wavelengths, provide minimal pulse broadening, be corrected for infrared wavelengths, and have a suitably long-working distance for imaging thick samples. Luckily, many of the confocal microscope manufacturers are now making very good lenses suitable for two-photon microscopy, so finding suitable lenses is not as difficult as it was in the past.

8.4 Spinning Disk Systems

Unlike laser scanning systems, where the image is formed by moving a diffraction-limited spot of laser light across the object plane of the specimen in a raster pattern, in spinning disk systems, the image is generated by the simultaneous illumination of multiple spots in the object plane. Each spot is generated by a series of micro-lens or pinhole apertures in a rapidly spinning disk (Chap. 1, Fig. 1.2).

8.4.1 The Nipkow Disk

In 1884 two seminal events in the progress of the development of light microscopy occurred. At about the same time as Abbe (1884) published his milestone work which provided the basic foundation for modern light microscopy, a young student in Germany, Paul Nipkow (1884), discovered how to encode a two-dimensional optical image into an electrical signal that could be transmitted as a one-dimensional or serial, time-dependent signal, similar to that of Morse code. This signal could then be transmitted over a single cable. Prior attempts at accomplishing this feat had resulted in the development of a highly complicated apparatus requiring multiple detectors and cables which gave very limited results. Nipkow's genius in solving this problem was to dissect the image by scanning it in a raster pattern using a spinning disk. The disk was opaque to light except where perforated with a series of rectangular holes spaced under specific geometrical conditions. The holes in the disk were placed at a constant angle relative to the center of the disk and at a constant, progressively decreasing radius to generate the raster pattern. Such a geometrical arrangement of apertures in the disk constitutes an Archimedes spiral (Fig. 8.7a). When such a disk is rotated at a constant velocity, the brightness of each image element passing through the apertures in the disk produces an image in a raster pattern. The brightness or intensity of each image element is essentially constant along the radii from the center to the margin of the disk. In addition, the arrangement of the pinholes describes the image as parallel concentric raster arcs. The arc of the pinholes also progressively traces out the image as adjacent parallel straight lines along the radii at any given X-Y position over the specimen. The

image output resulting from the raster pattern is captured by an appropriate device such as a charge-coupled device (CCD) camera.

The arrangement of the pinholes defined by the Archimedes spiral results in a pattern which expresses equal peripheral pitch along the spiral pattern of the pinholes. In addition, the pattern produces equal radial pitch which results in equal illumination and scanning independent of the radius and rotation speed of the disk. Thus, there is minimal to no distortion of the image when it is obtained by the Archimedes spiral arrangement of pinholes in the Nipkow disk.

Alternate patterns of pinholes in the spinning disk are unsatisfactory for confocal image acquisition. When the pinholes are arranged in an equal fixed angular spiral or circular pattern, the light intensity at the outer margin of the disk is less than that in the inner regions of the disk. This unequal distribution of light intensity across the disk is the result of the pitch between the pinholes becoming wider toward the outer margin of the disk. The increased pitch results in an increasing distance between the pinholes at the periphery of the disk. Thus, in a given unit of time, fewer pinholes collect light information at the outer margin of the disk resulting in progressive degradation of the image in this region. If the pinholes are arranged in an equally spaced tetragonal pattern, there is no loss of light intensity across the disk. Since the pinholes are equally spaced, there is no imbalance of light intensity between the inner and outer peripheries of the disk. However, when the disk is rotated, the scanning pitch of the pinholes is not equal which results in the generation of light and dark stripes across the image (Tanaami et al. 2002).

The modern Nipkow disk (Fig. 8.7b) consists essentially of two major components. The core of the disk is an optically flat glass disk which is rigid enough to withstand rotation speeds of up to 2000 rpm. On this glass disk, the Nipkow arrangement of pinholes is produced by photolithographic methods. This surface consists of a reflecting black chrome layer (< 1.0 μm thick) with a reflectivity of only a few percent laid down on a glass disk. The most important criteria in the design of the Nipkow disk for confocal microscopy are the size and spacing of the pinholes.

8.4.2 Nipkow Disk Pinhole Size

In spinning disk systems, collimated light impinges on the disk and the effective aperture of the light rays entering the microscope objective lens are determined by diffraction at the disk pinhole. The magnitude of diffraction by the pinhole is a function of the light wavelength and pinhole size (R-radius). Calculations have demonstrated that resolution in the Z direction (d_z) is directly proportional to the square of the radius (R) of the pinhole (Kino 1995). If the pinholes in the disk are too small, loss of illumination intensity by light rays being diffracted outside of the objective lens aperture occurs, and image information from emitted photons is lost as these photons are not able to enter the pinhole (Fig. 8.8a).

When the pinholes are too large (Fig. 8.8b), resolution of the image in the X-Y and Z directions is significantly reduced. In this case, the collimated light rays

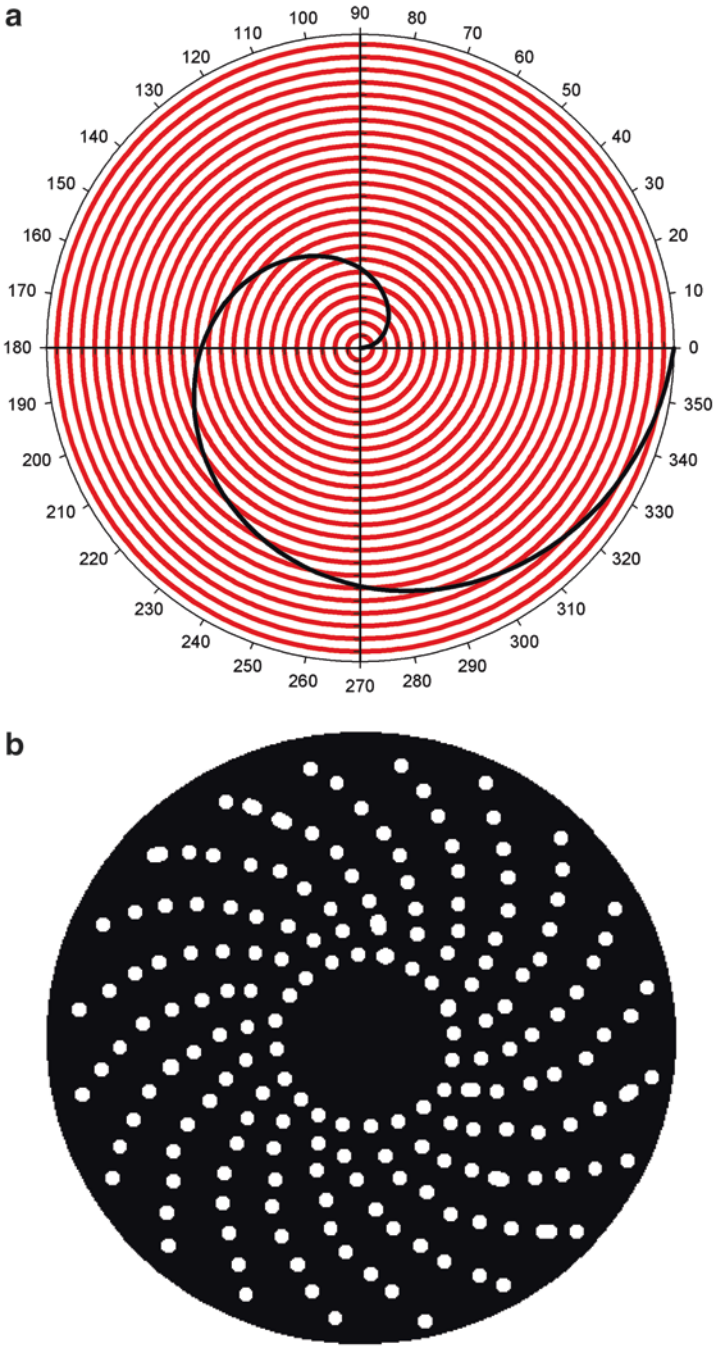

Fig. 8.7 The Archimedes spiral. (**a**) shows the Archimedes spiral plotted in polar coordinates (black line). When pinholes are place on the Archimedes spiral at the intersections of the black and red lines and the Archimedes spiral rotated the pinholes sweep out concentric parallel raster lines (red lines). When multiple Archimedes spirals are present the entire image field is continuously scanned without the presence of intervening scan lines. (**b**) shows a modern Nipkow disk which is a blackened glass disk with pinholes arranged in Archimedes spirals

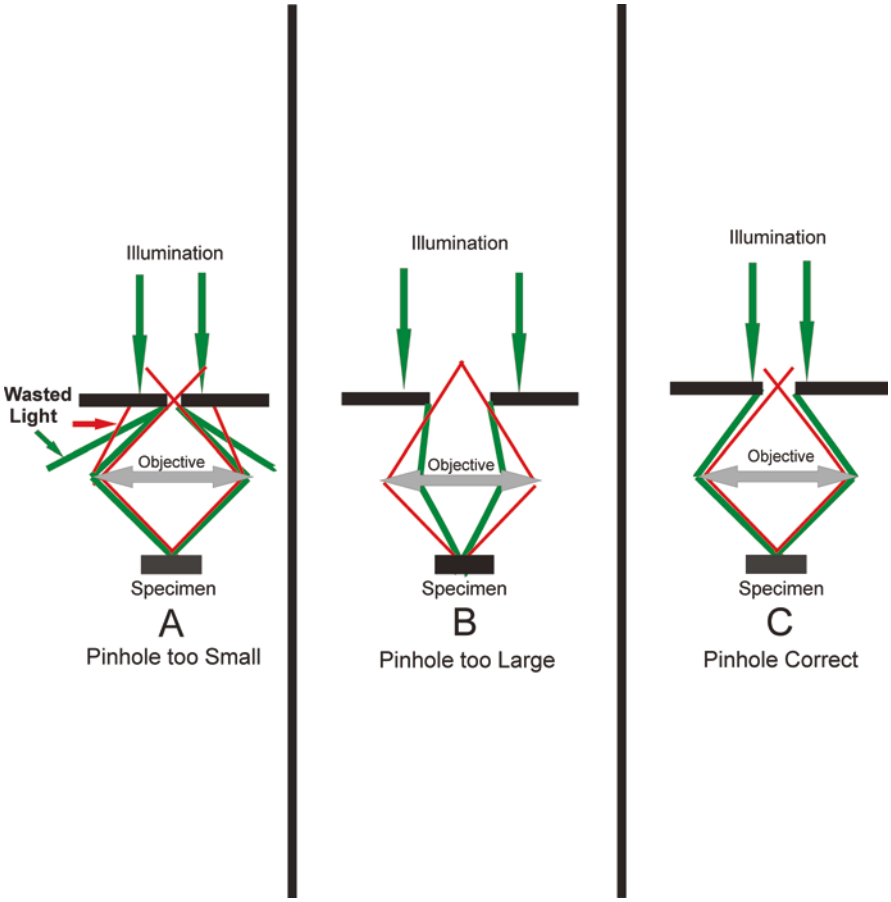

Fig. 8.8 Effect of Nipkow disk pinhole size (diameter) in Nipkow disk on image quality. In (**a**) the pinhole in the Nipkow disk is too small. Image quality is degraded by loss of higher-order diffracted light rays not being collected by the pinhole. In (**b**) the pinhole in the Nipkow disk is too large. Image quality (resolution) is lost because the light rays are insufficiently diffracted and do not completely fill the aperture of the objective. In 8.78 the pinhole in the Nipkow is of the proper radius. Under these conditions diffracted light from the pinhole fills the aperture of the objective, and the refracted or light emitted by the specimen is maximally collected by the pinhole

which enter the pinhole aperture are diffracted into a relatively narrow beam which does not completely fill the aperture of the objective lens. This causes the objective lens to function at a lower NA than designed for and results in loss of image resolution. In addition, emitted light from the specimen may not enter the appropriate pinhole. This results in further loss of resolution in the X-Y and Z directions (Fig. 8.8b). In a pinhole of correct size (radius), the diffracted light from the pinhole fills the objective aperture, and the refracted light from the specimen is maximally collected by the pinhole (Fig. 8.8c).

An equation which estimates the optimal pinhole radius was derived from the Fraunhofer diffraction theory for a circular aperture in the focal plane of the objective (see Goodman 1968; Xiao and Kino 1987; Kino and Xiao 1990 for details of the equations and assumptions used). The optimal pinhole radius is determined by the following equation:

$$R_o = \frac{0.25\lambda M}{\mathrm{NA}}$$

where λ is the wavelength of the light used, M the magnification, and NA the numerical aperture of the objective. This equation is applicable to microscopes of fixed tube length and infinity-corrected optics. The R_o value for a 100×, 1.4NA oil immersion objective with light at a λ of 546 nm is 9.75 um, and for a 10× (0.5 NA) objective under the same conditions, R_o is 2.73 um. This indicates that the ideal situation would require an individual disk with the appropriate sized pinholes to match each objective on the microscope. Since pinholes of these ideal sizes would result in a significant loss of illumination (1% transmitted light or less) and require multiple disks in a system, alternate approaches have been employed.

In general, a single disk is used with the optimal R_o value chosen to match the objective lens with the highest magnification and NA. The pinhole size used in early experimental designs of spinning disk microscopes was usually 10um. Under this design criterion, the pinhole diameter is larger than optimal for the objectives with lower magnification and NAs resulting in proportional loss of resolution at these magnifications. However, this loss of resolution for the lower magnification objectives may be acceptable if specimen resolution is less critical in this range of magnification. If R_o becomes very large, out-of-focus information in the Z-plane contributes to the image, and the system is no longer confocal and becomes a standard fluorescence microscope. Most modern commercially available Nipkow confocal systems (Yokogawa systems) use a pinhole with a R_o of 20–25 um to insure the collection of sufficient light intensity for observation and image collection. This sacrifices some high-end resolution with high NA objectives, and there is a similar loss of resolution at low magnification. Loss of signal and resolution are often criticisms of spinning disk confocals, but these compromises are balanced by the speed of imaging for live cell applications.

8.4.3 Nipkow Disk Pinhole Spacing

The Archimedes spiral of a spinning disk is governed by the simple polar equation:

$$r = a + b\theta$$

The parameter a refers to the turn of the spiral, and b is the distance between successive turnings. In the Archimedes spiral, the successive turns have a constant separation distance which is equal to $2\pi b$ when θ is measured in radians. Applying

this to the Nipkow disk for confocal microscopy, identical pinholes are laid out circumferentially on the rotational arm of an Archimedes spiral at a constant angle (θ) and constantly increasing distances (r) from the center of the disk. Multiple Archimedes spiral arms are present on the Nipkow disk resulting in 20,000–200,000 pinholes depending on the size and manufacturer of the disk.

As the spacing between adjacent pinholes in the disk is decreased, the pinholes become too close together, and the aggregate area of the pinholes approaches the total area illuminated. Under these conditions, the signal intensity emitted from the specimen no long decreases sharply with the defocus distance characteristic of the objective lens. Instead, a portion of the out-of-focus light emitted by the specimen can return to the detector through alternate adjacent pinholes leading to loss of intensity and image resolution. An additional problem also arises when spacing between the pinholes is too small. Here the closeness of the pinholes, equal to or less than 5 pinhole radii apart, can result in interference between images resulting in a speckle effect. This is especially true when a monochromatic laser and narrow band-pass filter are used as the excitation source. This phenomenon can be minimized by the use of a diffuser or phase randomizer placed in front of the illumination source.

Spacing of the pinholes too far apart results in uniform loss of excitation light intensity to the specimen and emitted light from the specimen. Both result in a deterioration of overall image quality.

The ideal spacing of the pinhole along the arch of the Archimedes spiral is a function of the magnification, NA, and Z defocus distance characteristic of the objective lens. Here, as with the size of the pinhole, compromises have been made in pinhole spacing to reduce the complexity of the mechanism and moderate the cost of the instrument. A current typical Nipkow disk has a pinhole spacing of 253 um based on high-magnification (100×), high-resolution (NA = 1.4) immersion objectives. With objectives of lower magnification and NA, the ideal pinhole spacing increases in distance (Fig. 8.9). This adjustment of the pinhole spacing does not produce a significant loss of image resolution provided the emitted light rays from the specimen are focused on the pinhole. However, there is loss of both excitation and emission light intensities with low magnification and NA objectives and short pinhole spacing.

8.4.4 The Petran Microscope

The initial application of the Nipkow disk to optical microscopy was the development of the Tandem Scanning Reflected Light Microscope (TSRLM) by Petran and his co-workers (Petran et al. 1968, 1985). Here the disk is perforated with many holes laid down along the path generated by a multiple set of interweaving Archimedes spirals. The pinholes are separated by a distance large enough so that there is no interaction between the images formed by the individual pinholes. The complete image is formed by moving the pinholes (spinning the disk) so as to fill the

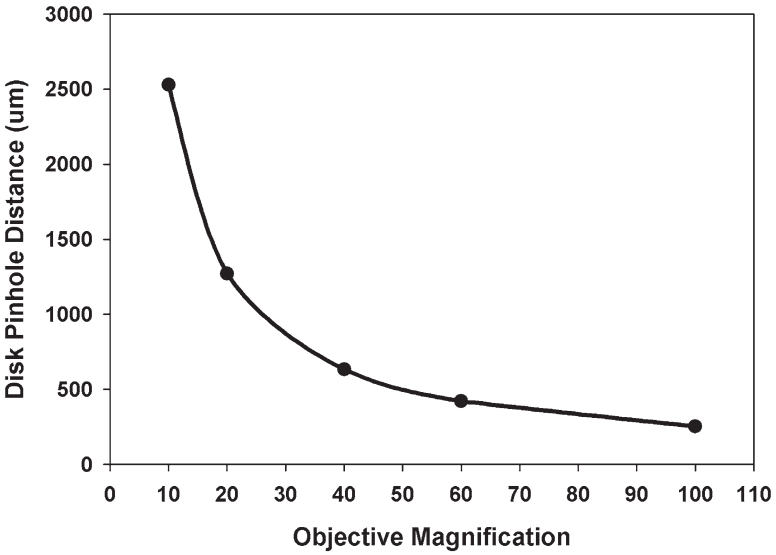

Fig. 8.9 Relationship between ideal pinhole spacing and magnification power of the microscope objectives

space between them. Although TSRLM had the advantages of real-time imaging and good cross-sectioning ability, it possessed numerous disadvantages which limited its usefulness. The most serious problems were a poor light budget with only about 1% of the light being useful, complicated mechanical components which were required to reduce internal reflection from the disk, and considerable difficulty in maintaining the alignment of the large number of optical components required for operation of the system.

8.4.5 The Xiao and Kino Microscope

The next advance in spinning disk-based confocal microscopy was the development of the real-time scanning optical microscope (RSOM) which is able to detect light from the same pinhole from which a given area of the specimen is illuminated (Xiao and Kino 1987; Xiao et al. 1988). This is accomplished by constructing a disk of highly reflective black chrome. The surface of the disk produces a reflected beam which is easily eliminated by an optical stop. The disk is also tilted and the optical stop placed in a position where the light reflected from the disk is focused (Xiao et al. 1990). Tilting of the disk can distort the image due to defocusing of the pinholes near the edge of the field of view. Typically, for a few degrees of tilt, the distortion is minimal. However, when imaging requires high-resolution or extremely accurate metrology, tilting of the disk is inappropriate, and other systems must be used.

Additionally, to further reduce interference by reflected light, the light from the source is polarized and light reaching the eyepiece observed through an analyzer with its plane of polarization rotated 90° to the polarized source. A ¼ wave plate is placed in front of the objective lens so that light reflected from the plane of polarization is rotated 90°, so it can be observed through the eyepiece (Fig. 8.10). This set-up and orientation of optical components enhance the SNR in the image. However, because fluorescent light emitted from a fluorescently labeled specimen is randomly polarized, a small fraction of the desired signal is also eliminated from the image.

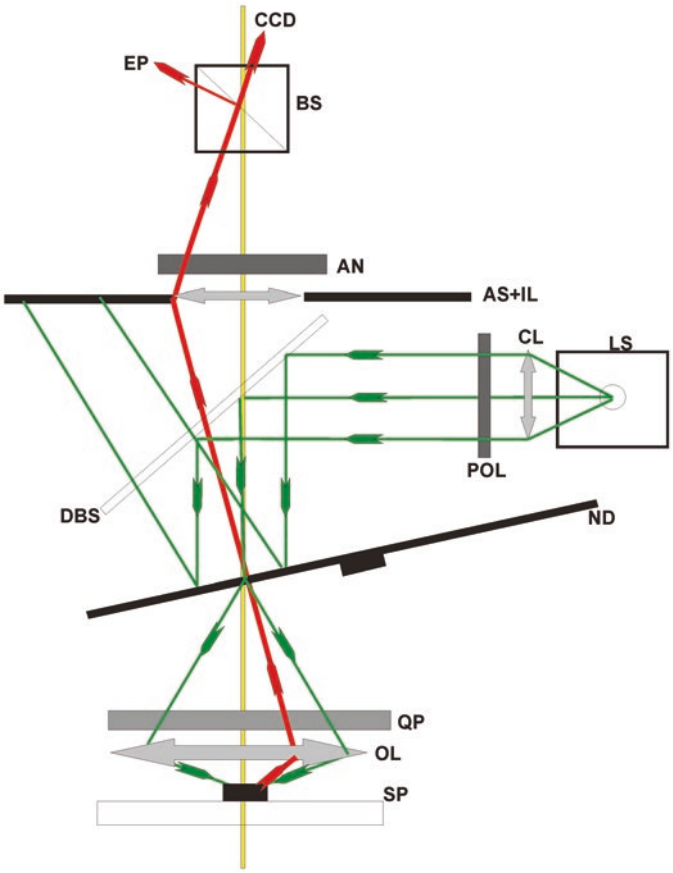

Fig. 8.10 The tilted Nipkow disk confocal microscope. The design of Xiao and Kino. In this design, the Nipkow disk is tilted to eliminate reflected incident light from the disk from interfering with light emitted by the specimen. Diagram traces the ray path for incident and emitted light interacting with one pinhole. Green lines, incident light from light source (LS); red line, emitted light by the specimen (SP); yellow line, optic axis of the microscope. Components: LS light source, CL collecting lens, Pol polarizer, DSB dichroic beam splitter, ND Nipkow disk with pinholes, QP quarter-wave plate, OL objective lens, Sp specimen, AS+ IL aperture stop and intermediary lens, BS bean splitter, EP eyepiece; CCD-CCD camera

This loss of fluorescent signal can be minimized by setting the polarizer and analyzer to a parallel orientation. Additionally, for fluorescence, the reflected light from the disk can be removed by a dichroic beam splitter and a barrier filter.

In real time the illumination of the specimen is accomplished by use of relatively broadband light. This results in low temporal coherence and minimal speckle effects which arise from interference between neighboring layers within the specimen or between reflections from the specimen and reflecting components within the microscope. Because of the low transmittance of light through the disk, light sources of high intensity such as mercury or xenon arc sources, or more recently metal-halide lamps, are used. Metal-halide lamps are particularly useful in this application since they emit at essentially constant illumination power across the objective field.

Application of Kohler illumination to the spinning disk configuration also improves the image quality. Each point on the source is focused to a point in the back focal plane of the objective lens when the disk is not present. When the disk is introduced into the optical path, Kohler illumination insures that the central axis of the diffracted beams passing through the individual pinholes all pass through the center of the back focal plane of the objective. This configuration gives uniformity to the illumination and optimizes resolution over the field of view.

8.4.6 The Corle Microscope

The design of the spinning disk confocal microscope by Corle et al. (1991) further improved image quality by eliminating the tilt of the Nipkow disk and improving the overall optical path of the excitation and emission photons. The initial improvement came by selectively isolating the most stable portion of the mercury or xenon arc light source. These light sources exhibit an inherent instability across the arc, especially at the margins. The most stable portion of the arc is the central region directly between the electrodes. In this microscope design, the spot of maximal intensity of the arc near the cathode is isolated by imaging it on to a pinhole aperture by the condenser lens. This concentrates the maximal intensity of the light source into a bright, essentially point source of illumination. This makes the illumination as uniform as possible across the field of view. The illumination in the plane of the Nipkow disk is collimated by the addition of a collecting lens behind the pinhole aperture. Before reaching the Nipkow disk, the collimated rays of light are further refined by the addition of a field stop to remove aberrations from the outer edge of the illumination and to define the size of the field to be illuminated.

A polarizer is then placed in the collimated beam to eliminate spurious reflected light in the system. The polarizer and analyzer in the Corle system are analogous to that used in the RSOM described above. Light exiting from the polarizer is focused onto a 90° beam splitter and the Nipkow disk as a collimated beam of light by a secondary objective lens. The diffracted light from the pinholes of the Nipkow disk is passed through a field lens situated just below the disk. This lens serves to minimize vignetting which produces darkening of the edges of the image field as a result

of light falling outside of the aperture of the lower objective lens. This field lens focuses the central rays of the diffracted beam to the center of a tube lens which collimates the beam to the aperture of the lower objective. This in turn focuses the light onto the specimen (Fig. 8.11). The light emitted by the specimen passes back through this lens system and the pinhole of the Nipkow disk where it is focused by the secondary objective as a collimated beam. This collimated light then passes directly through the dichroic beam splitter, a field stop, and the analyzer and is focused by a tube lens to the eyepiece for direct viewing or to an appropriate camera for image collection.

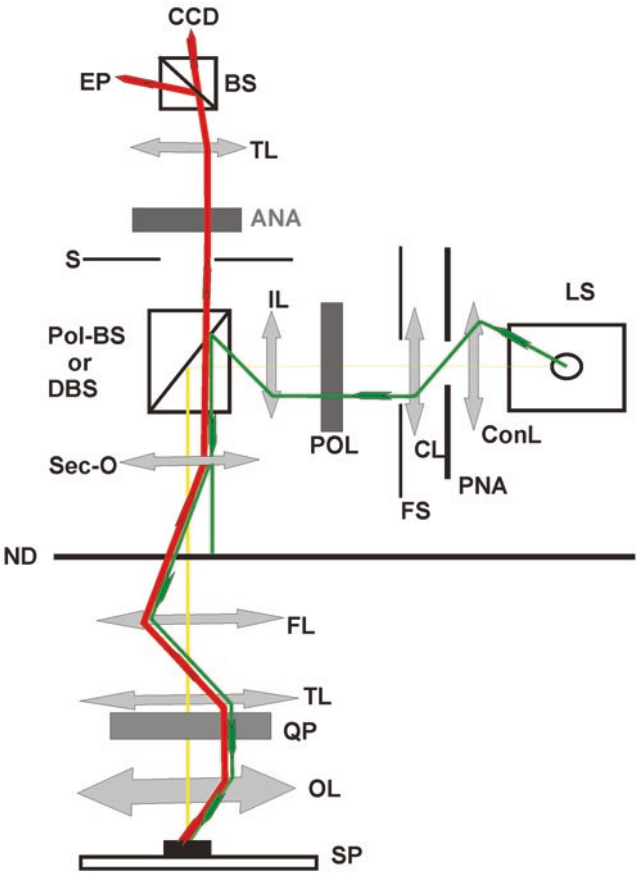

Fig. 8.11 Nipkow spinning disk microscope: Corle design. Diagram traces the ray path for incident and emitted interacting with one pinhole. Green lines, incident light from light source (LS); red line, emitted light by the specimen (SP); yellow line, optic axis of the microscope. Components: LS light source, Cond L condenser lens, PHA pinhole aperture, Col L collimating lens, FS field stop, Pol polarizer, IL intermediary lens, Pol-DSB polarized or dichroic beam splitter, SO secondary objective, ND Nipkow disk with pinholes, FL field lens, TL tube lens 1, QP quarter-wave plate, OL objective lens, Sp specimen, AS aperture stop, Ana analyzer, TL-2 tube lens 2, BS bean splitter, EP eyepiece, CCD-CCD Camera

8.4.7 The Yokogawa Spinning Disk Confocal Microscope

Although spinning disk confocals can obtain images at a very rapid rate, the need for a nonoverlapping spacing (described above) means that a large area of the disk lacks openings. Thus, only a small portion of the available light is used to illuminate the specimen. A significant improvement was made on the spinning disk confocal microscope by the addition of a second spinning disk which contains an array of micro-lenses (Ichihara et al. 1996; Nakano 2002; Genka 1999) which collect and focus more of the available light into the pinholes. This design forms the bases of the compact confocal scan head developed by Yokogawa (Yokogawa Electric Corp). Yokogawa confocal heads are currently used by several confocal manufacturers including PerkinElmer and VisiTech.

In this system, the scanning portion contains a dual spinning disk arrangement in which the first disk has an array of 20,000 micro-lenses arranged in an Archimedes spiral. The micro-lenses of this disk receive the illumination light and are accurately aligned with a corresponding array of pinholes on the second, Nipkow, disk. The micro-lens array disk and the Nipkow disk are physically fixed at a distance equal to the focal length of the micro-lenses and are rotated together so as to scan the field of view at high speed. The typical speed of scanning of this dual disk system is 1800 rpm (30rps) which results in 1200 pinholes scanning the sample at any given time. These spinning rates are 12 times the video rate of 30fps which results in a 12-frame average for each video image.

The constant pitch Archimedes spiral arrangement of the micro-lenses in the first disk and pinholes in the Nipkow disk creates even illumination across the image field without creating scanning artifacts. Light from the laser or arc lamp illumination source is collimated and projected on to the micro-lens array disk. Light focused by the micro-lenses passes through a dichroic beam splitter mounted in the space between the micro-lens and Nipkow disks and enters the corresponding pinhole in the Nipkow disk. First focusing the illumination light by the micro-lens disk prior to it passing through the Nipkow disk improves available illumination at the specimen by about 40%. The incident light is diffracted by the pinhole to fill the aperture of the objective lens where it is focused onto the focal plane of the specimen. Light emitted from the specimen is collected by the objective lens and then focused back on to the pinholes in the Nipkow disk. Transmission of the emitted light from the specimen through the same pinholes in the Nipkow disk eliminates out-of-focus signal and results in a confocal image.

Emitted light from the pinholes in the Nipkow disk is then deflected by a dichroic beam splitter positioned between the Nipkow disk and the upper micro-lens array disk and focused on the appropriate detector (Fig. 8.12). This arrangement of disks has several advantages including the improved light efficiency described above. This has real advantages for real-time confocal imaging of live cells where fluorescence emission is often limiting. The improved light efficiency allows fluorescence imaging to be carried out at low intensity and power per unit area thus reducing or minimizing photobleaching of probes and related phototoxic damage to living cells.

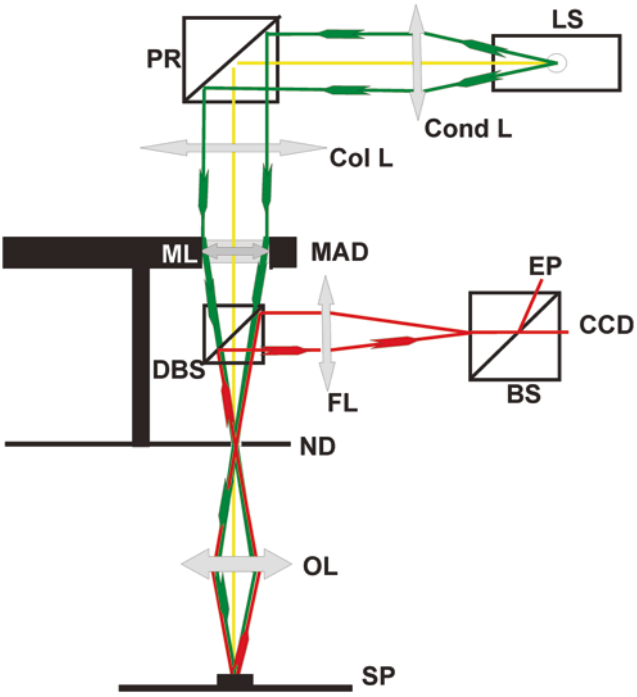

Fig. 8.12 Nipkow spinning disk microscope: Yokogawa design. This design represents a significant improvement over pervious spinning disk microscopes. The principle improvement is the use of a tandem spinning disk system in which the pinholes in the upper disk contain micro-lenses which focus the incident light on to the pinholes in the Nipkow disk. Diagram traces the ray path for incident and emitted interacting with one microlens in the microlens array disk and one tandem pinhole in the Nipkow disk. Green lines, incident light from light source (LS); red line, emitted light by the specimen (SP); yellow line, optic axis of the microscope. Components: LS light source, Cond L condenser lens, PR 90° reflecting prism or front surface mirror, Col L collimating lens, MAD microlens array disk, ML micro-lens, DBS dichroic beam splitter, ND Nipkow disk with pinholes and tandem with microlens array disk, OL objective lens, Sp specimen, FL field lens, BS beam splitter, EP eyepiece, CCD-CCD Camer

By focusing the incident light onto the pinholes in the Nipkow disk, backscatter of the incident light at the surface of the Nipkow disk is also significantly reduced improving the SNR of the confocal image. Improved speed of imaging is also possible with frame scan speeds as high as 1000 frames per second possible.

8.4.8 Slit Scanning Systems

A modification of the pinhole type of spinning disk is the slit scan spinning disk which Olympus has introduced in their Disk Scan Unit (DSU) systems. The DSU systems offer a choice of five exchangeable disks with different slit widths for use

with different objectives and specimen thicknesses. This addresses many of the problems discussed above concerning matching of objectives and pinhole aperture for optimum resolution. As discussed above for the swept field slit scanning systems, the point spread function is affected when using slits rather than pinholes, so there is still some sacrifice of resolution, but the overall combined confocal effect and speed of imaging is superior to epifluorescent microscopes.

8.4.9 Image Collection in Spinning Disk Systems

Images generated by spinning disk systems can be viewed directly by looking through a port on the scan head or captured by using the appropriate recording device. Since images are collected at high speed and may also have low SNR levels, CCD or EMCCD cameras remain the most appropriate collection devices in these situations although newer sCMOS cameras are rivaling CCD systems. Although very reliable and inexpensive CCD cameras are available, imaging of live cells using fluorescence microscopy requires very sensitive and thus more expensive CCD cameras. Depending on the spinning disk system, images may be generated at rates between 300 and 1000 frames per second. The actual speed at which the instrument can capture images is dependent on the speed and sensitivity of the attached CCD camera and the intensity of the fluorescent emission signal from the specimen. When high-speed imaging is required, the faster frame rates of CMOS cameras become an advantage. Image collection using sensor arrays such as CDC and CMOS cameras was discussed more fully in Chap. 6. Different experimental applications may require image acquisition at varying speeds or frame rates. The speed of the device is determined by the pixel read rate and the number of pixels which comprise the image.

Literature Cited

Abbe E (1884) Note on the proper definition of the amplifying power of a lens or lens system. J Roy Microsc Soc 4(2):348–351

Centonze V, White J (1998) Multiphoton excitation provides optical sections from deeper within scattering specimens than confocal imaging. Biophys J 75:2015–2024

Corle TR, Mallory CL, Wasserman TD (1991) Improved confocal scanning microscope. U.S. Patent 5,067,805, 26 Nov 1991

Denk W, Strickler J, Webb W (1990) Two-photon laser scanning fluorescence microscopy. Science 248:73–76

Denk W, Piston D, Webb W (1995) Two-photon molecular excitation in laser-scanning microscopy. In: Pawley J (ed) Hanbook of biological confocal microscopy, 2nd edn. Plenum, New York, pp 445–458

Gauderon R, Lukins P, Sheppard C (1999) Effect of a confocal pinhole in two-photon microscopy. Microsc Res Tech 47:210–215

Genka C, Ishida H, Ichimori K, Hirota K, Hirota Y, Tanaami T, Nakazawa H (1999) Visualization of biphasic Ca^2 diffusion from cytosol to nucleus in contracting adult rat cardiac myocytes with an ultra-fast confocal imaging system. Cell Calcium 25:199–208

Gerritsen H, deGrauw C (1999) Imaging of optically thick specimens using two-photon excitation microscopy. Microsc Res Tech 47:206–209

Goodman JW (1968) Introduction to fourier optics. McGraw Hill, New York

Göppert-Mayer M (1931) Uber Elementarakte mit zei Quantenspruengen. Ann Physik (Berlin) 9:273–294

Ichihara A, Tanaami T, Isozaki K, Sugiyama Y, Kosugi K, Mikuriya K, Abe M, Umeda I (1996) High-speed confocal fluorescence microscopy using a Nipkow scanner with microlens for 3-d imaging of a single fluorescent molecule in real time. Bioimages 4:57–62

Kino GS (1995) Intermediate optics in Nipkow disk microscope. In: Pawley JB (ed) Handbook of biological confocal microscopy. Plenum Press, New York, pp 155–165

Kino GS, Xiao GQ (1990) Rea-time scanning optical microscopes. In: Wilson T (ed) Scanning optical microscopes. Pergamon Press, London, pp 361–387

Laine RF, Kaminski Schierle GS, van del Linde S, Kaminski CF (2016) From single-molecule spectroscopy to super-resolution imaging of the neuron: a review. Methods Appl Fluoresc 4:02204

Leung BO, Chou KC (2011) Review of super-resolution fluorescence microscopy for biology. Appl Spectrosc 65(9):967–980

Nakano A (2002) Spinning-disk confocal microscopy—a cutting edge tool for imaging of membrane traffic. Cell Struct Funct 27:349–355

Nipkow P (1884) German Patent no. 30,105. Germany

Petran M, Hadravsky M, Egger MD, Galambos R (1968) Tandem scanning reflected light microscope. J Opt Soc Am 58:661–664

Petran M, Hadravsky M, Boyde A (1985) The tandem scanning reflected light microscope. Scanning 7:97–108

Piston D (1999) Imaging living cells and tissues by two-photon excitation microscopy. Trends Cell Biol 9:66–69

Sydor AM, Czymmek KJ, Puchner EM, Mennella V (2015) Super-resolution microscopy: from single molecules to supramolecular assemblies. Trends Cell Biol 25(12):730–748

Tanaami T, Otsuki S, Tomosada N, Kosugi Y, Shimizu M, Ishida H (2002) High-speed 1 frame/ms scanning confocal microscope with a microlens and Nipkow disk. Appl Opt 41:4704–4708

Xiao and Kino (1987) A real-time confocal scanning optical microscope. In: Wison T, Balk L (eds) Proceedings SPIE, vol. 809, Scanning Imaging Technology, pp 107–113

Xiao GQ, Corle TR, Kino GS (1988) Real time confocal scanning microscope. Appl Phys Lett 53:716–718

Xiao GQ, Kino GS, Masters BR (1990) Observation of the rabbit cornea and lens with a new real time confocal scanning optical microscope. Scanning 12:161–166

Yamanaka M, Smith NI, Fujita K (2014) Introduction to super-resolution microscopy. Microscopy 2014:177–192